

Chapter 5

Characterisation of specific metabolic responses identified in the transcriptomic and proteomic investigations of AdoMetDC inhibition in *P. falciparum*

5.1 Introduction

The “omics” technologies as a stand alone do not always provide sufficient information for a complete understanding of the physiology and pathogenicity of an organism (Hegde *et al.*, 2003). It is therefore of utmost importance to integrate the “omics” technologies to gain maximal information in understanding a response of an organism upon any perturbation. Unfortunately, integration of transcriptomic and proteomic data is not always easy since a clear correlation between mRNA and protein abundance is not always the case (Gygi *et al.*, 1999). It is therefore of utmost importance to determine such possible regulatory mechanisms. Another important aspect of integration of all the “omic” data is to determine the biological significance of the data that were obtained. In order to determine the biological significance of the transcriptomic (Chapter 4) and the proteomic (Chapter 3) data that emerged from *PfAdoMetDC* inhibition with MDL73811, several aspects were investigated further and include the possibility of hypermethylation as the mode-of-action of MDL7381. The interaction between AdoMetDC inhibition and the folate pathway was also further investigated. Finally, the metabolome was investigated to determine the regulation of metabolites within polyamine biosynthesis.

5.1.1 Transcriptional and translational control

mRNA abundance is not always proportional to protein expression due to RNA splicing and various protein modifications that include PTM's, protein degradation, protein turnover as well as differences between transcription and translation (Hegde *et al.*, 2003, Griffin *et al.*, 2002, Gygi *et al.*, 1999). In contrast to some other organisms, *P. falciparum* generally has good correlation between mRNA and protein levels although there might be a slight delay between mRNA and protein accumulation which is mostly regulated by post-transcriptional mechanisms (Le Roch *et al.*, 2004). The *P. falciparum* parasites utilises a process of stage-specific transcript production and therefore post-transcriptional regulation would form an integral part in regulation of transcriptional processes (Bozdech *et al.*, 2003). Investigation of transcription associated proteins within *P. falciparum* revealed 156 transcription associated proteins that may modulate mRNA and translation rates, which also suggests that protein expression is mainly regulated by post-transcriptional



mechanisms (Coulson *et al.*, 2004). Post-transcriptional regulation may be a major mechanism of the control of gene expression within the parasite throughout the various life stages of the parasite (Ponts *et al.*, 2010). This process is highly co-ordinated and may also play a role in the adaptability of the parasite to environmental stresses (Mackinnon *et al.*, 2009). Translational repression is a post-transcriptional regulatory mechanism which also plays an important role in stage-specific transcript production of the malaria parasite and therefore also has a key role in parasite development (Mair *et al.*, 2006) especially in female gametocytes (Braks *et al.*, 2008).

5.1.2 DNA methylation

DNA methylation is a modification that includes the transfer of a methyl group from AdoMet to the 5'-carbon of cytosine creating the fifth DNA base, 5-methyl cytosine (5mC), which is widespread in CpG islands (Jones & Laird, 1999, Gitan *et al.*, 2002, Caiafa & Zampieri, 2005). CpG islands are 0.5-2 kb regions that are rich in cytosine-guanine dinucleotides and are found at the promoter region of some human genes (Caiafa & Zampieri, 2005). DNA methylation in eukaryotes may be involved in the regulation of gene expression by the methylation of transcription factor binding sites, induction of heterochromatin formation, as well as a possible defence mechanisms against molecular parasites (Oakeley E.J., 1999).

Disruption of polyamine synthesis can lead to increased DNA, protein and lipid methylation (Goldberg B. *et al.*, 1999). AdoMet plays an integral role in the production of polyamines and acts as a methyl donor for nearly all methylation reactions that include DNA and protein methylation. Initially, it was proposed that *P. falciparum* does not contain any DNA methylation sites such as 5mC and 6mA (Triglia *et al.*, 1992). This theory was later disregarded with the discovery that 5mC, but not 6mA may be present in *P. falciparum* (Hattman, 2005). However, this was again contradicted when LC-MS demonstrated the absence of 5mC in *P. falciparum* gDNA (Choi *et al.*, 2006).

The principle of DNA methylation detection is based on the observation that unmethylated cytosine is converted to uracil and leaves methylated cytosine as it is. This is done by the use of sodium-bisulfite, and was first observed in the 70's by Shapiro (Shapiro R. *et al.*, 1970a, Shapiro R. *et al.*, 1970b). Since then, developments have taken place to increase the speed and efficiency of the reaction. Bisulfite treatment of DNA has recently been modified to obtain high speed (Shiraishi M. & Hayatsu H., 2004), and easy methylation detection (Yang A.S. *et al.*, 2004). Other types of DNA methylation detection include the use of reverse phase HPLC or LC-MS of which both are considered to be extremely sensitive and good detection. Immunology can also be used for



detection of methylation. The DNA is denatured and then immobilized onto a DEAE membrane and incubated with monoclonal antibodies that are directed against m5C. The monoclonal antibody can then be detected by fluorescence. A two coloured microarray can also be used to quantitatively detect methylation within CpG islands using a methylation specific oligonucleotide microarray to potentially scan the whole genome for CpG methylation (Gitan et al., 2002).

In Trypanosomes the rate of protein methylation increases with the concentration of AdoMet (Goldberg B. et al., 1999). Inhibition of Trypanosomal AdoMetDC with the irreversible AdoMetDC inhibitor, MDL73811, will result in an elevation of the AdoMet levels, hence resulting in hypermethylation of DNA, proteins and lipids (Goldberg *et al.*, 1999, Goldberg *et al.*, 1997b). Protein methylation is increased 1.5-fold in Trypanosomes when MDL73811 is added for the inhibition of AdoMetDC and when DFMO is added for the inhibition of ODC (Goldberg B. *et al.*, 1997). In *T. brucei rhodesiense* an elevation in AdoMet levels is associated with cell death due to hypermethylation (Xiao *et al.*, 2009).

5.1.3 Regulation of AdoMet levels

Another factor that may have an impact on DNA methylation is the regulation of AdoMet and S-adenosyl-L-homocysteine (AdoHcy) levels. AdoMet is the universal methyl donor. Methionine is converted to AdoMet by the action of AdoMet synthase. AdoMet is decarboxylated by AdoMetDC in the formation of decarboxylated AdoMet (dcAdoMet) and spermidine which is essential for polyamine metabolism. AdoMet is also crucial for methylation reactions with the by-product of methylation being AdoHcy, which is rapidly degraded by AdoHcy hydrolase. AdoHcy, which is implicated in cardiovascular disease, inhibits methylation reactions by the down-regulation of the methyltransferases (Nakanishi *et al.*, 2001, Zinellu *et al.*, 2007). Therefore the AdoMet:AdoHcy ratio is of importance to DNA methylation, since high AdoMet levels will result in hypermethylation, but in the presence of high AdoHcy DNA hypomethylation will occur.

This chapter investigates the impact of *PfAdoMetDC* inhibition with MDL73811 further. The methylation status and AdoMet homeostasis of Plasmodial parasites inhibited with MDL73811 is investigated. To further validate polyamine depletion as an essential drug target the effect of polyamine depletion is investigated on metabolite level as well as possible synergy within a folate depleted environment. Finally, the transcriptomic and proteomic data are combined in an effort to evaluate the regulatory mechanisms that may be induced upon *PfAdoMetDC* inhibition with MDL73811.



5.2 Methods

5.2.1 Culturing of parasites for the determination of the methylation status of MDL73811 treated parasites over time

Pf3D7 parasites were maintained *in vitro* in human O+ erythrocytes in culture media and treated with 10 μ M MDL73811 as described in section 2.2.3 and section 3.2.3. Parasites (5 ml) at 10% parasitemia and 5% hematocrit were used per sample and harvested at 4 time points ($t_1 = 16$ HPI, $t_2 = 20$ HPI, $t_3 = 26$ HPI, $t_4 = 34$ HPI) by centrifugation of the parasites at 2500 \times g for 5 min and then washed twice with PBS, after which the infected erythrocytes were stored at -80°C until use.

5.2.2 gDNA isolation from *P. falciparum* for the determination of the methylation status

The erythrocyte pellet (0.25 ml erythrocyte pellet from 5 ml culture) containing the parasites were used for gDNA isolation using the QIAquick DNA Blood Mini-Kit (QIAGEN) without saponin lysis. The kit is based on the principle that the infected erythrocytes are lysed by the addition of chaotropic salts, followed by the removal of the cellular debris by filtration. The pellets were removed from -80°C and thawed before the addition of 20 μ l Proteinase K (QIAGEN) to the blood pellets and then vortexed. This was followed by the addition of 40 μ l RNase A (Fermentas) to degrade any remaining RNA by cleavage of phosphodiester bonds. This mixture was vortexed and then 200 μ l Buffer AL (Proprietary, QIAGEN) was added, vortexed and incubated at 56°C for 10 min. Absolute ethanol (200 μ l) were added, mixed and then transferred to the mini-spin column and centrifuged for 1 min at 13 000 \times g. The column was transferred to a clean microfuge tube before the addition of 500 μ l buffer AW1 (Proprietary, QIAGEN) and centrifugation at 13 000 \times g for 1 min, followed by the addition of 500 μ l buffer AW2 (Proprietary, QIAGEN) and centrifugation at 13 000 \times g for 3 min. This was followed by drying of the membrane by centrifugation at 13 000 \times g for 90 s before the addition of 200 μ l SABAX water to the membrane which was incubated for 5 min before centrifugation at 8 000 \times g for 90 s. The gDNA concentration was measured on a Nanodrop-1000 using the ds DNA-50 setting for double-stranded DNA. This setting for double-stranded DNA uses an extinction coefficient of 50 ng-cm/ μ l for the determination of the DNA concentration. The 260/280 ratio measurement was also determined and was always above 1.8 in order to ensure DNA free of protein contamination.



5.2.3 South-Western immunoblot for methylation detection after MDL73811 treatment of Plasmodial parasites

The method followed was based on a previous method followed by Fisher *et al.*, 2004 for global methylation detection in *Entamoeba histolytica* (Fisher *et al.*, 2004). The Plasmodial gDNA for all 4 time points were denatured by boiling for 5 min and then cooled on ice for 5 min. Each sample (1000 ng) were loaded onto a positively charged nylon membrane (Roche) along with 10 μ l of 0.01 M 5-methylcytidine (Sigma) as negative control. The Dotblotter (Bio-Rad) was used to spot samples onto the membrane under vacuum. After sample loading the membrane was cross-linked on a UV transilluminator light (Spectroline TC-312 A) at 312 nm for 3 min. The membrane was then placed into a re-sealable plastic bag and blocked overnight at 4°C in blocking buffer (2% (w/v) BSA in PBS). The next morning the blocking buffer was discarded and 1:5000 of the mouse anti-5-methylcytidine monoclonal IgG (AbD Serotec, Oxford, UK) was added to 10 ml wash buffer (2% (w/v) BSA, 0.1% Tween-20 in PBS) and incubated overnight at 25°C with gentle agitation. The next morning the membrane was washed 6 times with wash buffer for 10 min each before the addition of the goat anti-mouse IgG horse radish-peroxidase (HRP)-conjugate (1:1000) (AbD Serotec, Oxford, UK) in wash buffer and left to incubate for 1 h at 25°C. This was followed by 6 wash steps of 5 min each with wash buffer, 4 wash steps of 5 min each with 0.1% Tween-20 and finally 3 wash steps of 5 min each with PBS. Finally, the membrane was incubated for 5 min with equal volumes (4 ml each) of Luminol/Enhancer solution and stable peroxidase solution (Supersignal West Pico Chemiluminescent substrate). The excess reagent was drained, and the membrane was exposed to Hyperfilm ECL X-ray film (Pierce) for 30 s in the dark. The X-ray was developed for 1 min in Universal Paper developer (Illford), rinsed briefly in water, and then fixed for 3 min with Rapid Paper Fixer (Illford). The film was again rinsed in water and left to dry before being scanned on the Versadoc-3000 using Quantity One 4.4.1 (Bio-Rad), with the following settings: Densitometry, X-ray film, Clear white TRANS, 0.5 \times Gain and 1 \times 1 Bin. The density of each spot on the X-ray film was calculated using Quantity One and then the ratio of UT/T were calculated.

5.2.4 Determination of polyamine-specific transcripts by the addition of methionine to parasite cultures

Pf3D7 parasites were maintained as described in section 2.2.3. A parasite culture of 5 ml were used during the treatments and done in biological duplicates. Treatment with methionine took place 4 HPI in the early ring stage, and harvested 24 h later in the trophozoite stage. A stock solution of methionine (100 mM) was dissolved in water before being added to the culture media. Methionine was analysed at 4 different concentrations (100 mM, 10 mM, 1 mM, 0.1 mM), and done in

duplicate. Parasites were harvested by centrifugation of the culture at $2500\times g$ for 5 min and then washed twice with PBS, after which the infected erythrocytes were stored at -80°C until use.

5.2.5 RNA isolation and cDNA synthesis of the metabolite treated parasites

RNA was isolated from UT and T parasites in an RNase free environment using a combined RNeasy Mini Kit (QIAGEN) and TRI-Reagent (Sigma) method, with the incorporation of DNase I on-column digestion (QIAGEN) as described earlier in Chapter 4 section 4.2.2. For the methionine-treated samples, 1 μg RNA was used for each individual sample. First strand cDNA synthesis was initiated using 1 μg RNA per sample, 25 pmol random primer nonamer (Inqaba), 15 pmol OligodT (dT_{25}) (Inqaba) and incubated at 65°C for 10 min, followed by 1 min at 4°C . After this incubation step, 6 μl $5\times$ SuperScript First-strand buffer, 10 mM DTT, and 200 U Superscript III Reverse Transcriptase (Invitrogen) were added, mixed and incubated at 25°C for 5 min, 50°C for 1 h, 70°C for 15 min and then 4°C until use. Contaminating RNA was removed by hydrolysis with the addition of 1 M NaOH, and 0.5 M EDTA, pH 8 to the reaction mixture and incubating at 65°C for 10 min. The cDNA were purified using the PCR Clean-up kit (Qiagen). The cDNA was subsequently eluted by the addition of 30 μl pre-heated RNase-free SABAX water (37°C) directly onto the membrane and incubated for 4 min before centrifugation at $13\ 000\times g$ for 90 s to elute the cDNA. The cDNA concentration and purity was measured on a Nanodrop-1000 (Thermo).

5.2.6 Quantitative real-time PCR of methionine-treated parasites

cDNA from the methionine-treated (T_{met}) and untreated samples (UT_{met}) were diluted to 0.65 ng/ μl with SABAX water for use in qRT-PCR. A standard curve was constructed from a dilution series of UT_{met} samples that contained the following dilutions: an undiluted sample, 1/10, 1/20, 1/50 and 1/100 dilutions. Lactate dehydrogenase (LDH) was used as household transcript and used to construct the standard curve. The reactions were performed in a 384-well plate using the Lightcycler 480 (Roche) as described in section 4.2.9. The fold change was calculated for each sample by comparing the UT_{met} samples to the T_{met} samples, and were then normalised to LDH that remained unchanged with methionine treatment.

5.2.7 Metabolite extractions for S-adenosylmethionine (AdoMet) and S-adenosylhomocysteine (AdoHcy)

Parasites were cultured *in vitro* and treated with 10 μM MDL73811 as described earlier in section 2.2.3 and 3.2.3. Two time points were taken (t_1 :16 HPI, t_3 :26 HPI). 20 ml cultures in triplicate were



used for each time point at 15% parasitemia and 5 % hematocrit. Cultures were centrifuged to a 1 ml pellet and the pellet was then washed 3 times with PBS and kept on ice. The pellet was transferred to a 2 ml microfuge tube. A portion of this pellet was diluted 1000-fold (1 μ l of the pellet with 999 μ l fixation solution) in fixation solution (4% (w/v) glucose, 10% (w/v) formaldehyde in a saline solution containing 10 mM Tris-HCl, 150 mM NaCl, 10 mM sodium azide, pH 7.3) that was used for Neubauer cell counting, and ultimately for normalisation of the cultures. A volume of 1 ml of a 10% perchloric acid (PCA) solution was added to the 1 ml pellet immediately after centrifugation and washing and vortexed vigorously to obtain a brownish colour before being placed at -70°C for at least 16 h. The samples were then thawed and again vortexed vigorously before being centrifuged at $16\ 000\times g$ for 10 min at 4°C . The supernatant were removed to a clean microfuge tube and then filtered using a $0.22\ \mu\text{m}$ HPLC filter (GE Healthcare) before 200 μ l injections were made onto the HPLC and stored at -70°C until use. HPLC analyses were performed on a Waters HPLC equipped with a Waters 600 pump, Waters 996 Photodiode Array detector and a Waters 717 Plus autosampler. High performance liquid chromatography was performed with a 250 mm x 4.0 mm Luna C18 (2) 5 μm reverse-phase (RP) column (Phenomenex). A Guard-PakTM Precolumn steel housing (Waters Corporation) with μ Bondapak C18 HPLC precolumn inserts (Waters Corporation) was connected in-line. Mobile phase A consisted of an aqueous solution of 8 mM octanesulfonic acid and 50 mM NaH_2PO_4 , mobile phase B consisted of 100% methanol. Mobile phase C consisted of only MilliQ water and mobile phase D consisted of 95% acetonitrile. The column were equilibrated with 80% A: 20% B before each injection, and upon injection of the sample maintained for 8 min, before being changed to 60% A: 40% B and maintained for 13 min after which the gradient was changed back to 80% A: 20% B and maintained until the end of the run (35 min in total). Absorbance measurements were made a 254 nm.

5.2.8 Malaria SYBR Green I-based fluorescence (MSF) assay for synergy determination of folates and MDL73811

The MSF assay was performed as described earlier in Chapter 3 section 3.2.1. The first column of the sterile 96-well plate was filled with only culture media and not used as part of the IC_{50} determination due to the possibility of edge effects. The second column contained $0.5\ \mu\text{M}$ CQ as a negative control, and represented total inhibition of parasite and hence no parasite growth. This was followed by the positive control that contained parasites in drug-free media. Folic acid were added to the folate-free media at normal physiological concentrations (23 nM) (Nduati *et al.*, 2008). This was also repeated with $1\ \mu\text{M}$ MDL 73811 (IC_{50}) added to the folic acid concentration range. To determine the presence of possible drug interactions, *Pf3D7* parasites were cultured in folic acid

deficient media containing pyrimethamine (PYR) and MDL73811. Pyrimethamine (Sigma) was added to folate-free media. A 10 mg/ml stock solution of PYR was prepared by dissolving 10 mg PYR in 1 ml DMSO, and then further diluted to a final concentration of 1.28 μ M in PBS. The IC_{50} for PYR was determined before the synergism study could commence. Serial dilutions were made of both drugs as they were added together. The plate was then placed into a gas chamber and gassed for 2 min, before being placed in a 37°C incubator for 96 h. On the day of the assay, SYBR green buffer was prepared and added (100 μ l) to each of the wells of a 96-well black fluorescence plate (Nunc) followed by 100 μ l of resuspended treated parasites. The plate was then incubated for 1 h in the dark at room temperature before the fluorescence was measured using the Fluoroskan Acent FL Fluorimeter (Thermo LabSystems) at excitation of 485 nm and emission 538 nm (integration time of 1000 ms). Data were analysed using SigmaPlot 9.0 to determine the IC_{50} of MDL73811 and PYR against *Pf3D7*.

To determine possible synergism between MDL73811 and PYR in folate-free media the drugs were added to the *Pf3D7* parasites in combination. The first column of the plate was filled with only culture media and not used as part of the IC_{50} determination due to the possibility of edge effects. The second column contained 0.5 μ M CQ as a negative control, and represented total inhibition of parasite and hence no parasite growth. This was followed by the positive control that contained parasites in drug-free media. The next eight columns contained a serial dilution of the drug starting at the highest concentration of 16 μ M MDL73811 to the lowest concentration of 0.125 μ M MDL73811 and similarly, 120 nM PYR down to 0.23 nM for the lowest concentration. The plate was then placed into a gas chamber and gassed for 2 min, before being placed in a 37°C incubator for 96 h. The plate was then treated as described previously. Data were analysed using SigmaPlot 9.0 to determine the IC_{50} of MDL73811 against *Pf3D7*.

Another measure to determine synergism is by the calculation of the fractional inhibitory concentration (FIC) as given in equation 5.1 (Vivas *et al.*, 2007). For the calculation of the FIC value most studies use IC_{50} values, although a more accurate representation would be the use of IC_{90} or even IC_{99} values (Fivelman *et al.*, 2004). The combination of two drugs will indicate that a FIC value of <0.5 is considered as synergistic, since it indicative of a 4-fold decrease in minimum inhibitory concentration (MIC) (Fivelman *et al.*, 2004). Synergy between two drugs can be defined as $FIC \leq 0.5$, additivity/indifference is defined $FIC >0.5$ to 4, and antagonism is defined as an $FIC < 4$ (Fivelman *et al.*, 2004, Hu *et al.*, 2002).

To calculate for possible interaction:



$$FIC50 = \left(\frac{IC50 \text{ Drug A comb}}{IC50 \text{ Drug A alone}} \right) + \left(\frac{IC50 \text{ Drug B comb}}{IC50 \text{ Drug B alone}} \right) \quad \text{Equation 5.1}$$

$$FIC50 = \left(\frac{IC50 \text{ Pyr comb}}{IC50 \text{ Pyr alone}} \right) + \left(\frac{IC50 \text{ MDL73811 comb}}{IC50 \text{ MDL73811 alone}} \right)$$

$$FIC50 = \left(\frac{7.2819 \text{ nM}}{14.1370 \text{ nM}} \right) + \left(\frac{0.9709 \text{ }\mu\text{M}}{0.9600 \text{ }\mu\text{M}} \right)$$

$$FIC50 = 0.515 + 1.011$$

$$FIC50 = 1.53$$

5.2.10 Primer design

Primers with melting points around 55°C and a product length of 150-170 were designed using Oligo 6.0. The T_m for the primers was calculated with T_m in the range of 55°C. Five primers were designed that include MAL13P1.214, PF11_0061, MAL13P1.56, PFE1050w, PFF1300w and are given in Table 5.2. Existing primers that were used are given in Table 5.1

Table 5.1: Existing primers used for proteomic validation

PlasmoDB ID	Set	Primer sequence (5' - 3')	Product length	T _m ^a (°C)
PFF0435w	OAT f	CAACTTTGGTCCATTCGTACC	165	58
	OAT r	GCTACACCTGGGAAATAACTATC		59
PF13_0141	LDH f	GATTTGGCTGGAGCAGATGTA	169	58
	LDH r	CAACAATAATAAAAGCATTGGACAA		55
PFD0285c	LDC f	AGA GGG ATA TGG ATT GGT AGA	161	56
	LDC r	TTC TCT TCA TGT ATG ATA CAG TA		54
PF10_0322	AdoMetDC/ODC f	AATCAATTCCATGACGCTTATCTG	165	58
	AdoMetDC/ODC r	ACAATTCACCATTCTGTATCTTC		58
PFE0505w	Cyclo f	AAT TCT TTG ACC ATC TTA ATC ATT C	167	55
	Cyclo r	CAA AAC AAT TTT ACT TCC TTG GGT TA		57
Pfi0320w	ARG f	CGT TTC CAT TAT TGG TTC TC	164	53
	ARG r	GTT TCA TTT CAT TAT CCC CAT TAT C		56
PFI1090w	SAMS f	TTT AGA TTA CAA AAC GGC AGA GAT AA	160	57
	SAMS r	AGG CAT ATA ATT CTC AGT TTC ATC AG		58

$$^a T_m = 69.3 + (0.41 \times \%GC) - \left(\frac{650}{\text{Primer length}} \right) \quad \text{(Rychlik et al., 1990)} \quad \text{Equation 5.2}$$

5.3 Results

5.3.1 Methylation status of *PfAdoMetDC* inhibited parasites

The action of MDL73811 upon AdoMetDC in Trypanosomes were speculated to be through hypermethylation of nucleic acids or proteins, therefore resulting in parasite death (Bacchi *et al.*, 1992a). To investigate the possibility of hypermethylation of genomic DNA (gDNA) in Plasmodial parasites, gDNA of Plasmodial parasites were isolated and prepared for an immunoblot that is able to detect 5mC within gDNA (Fisher *et al.*, 2004). Methylated RNA is able to interfere with detection of 5mC in gDNA and therefore RNA was removed from the samples with RNase A. Four time points were chosen for the detection of possible methylation of gDNA in AdoMetDC inhibited samples to determine the possibility that methylation might increase over time. gDNA (1000 ng) for each time point was quantitatively loaded onto the positive nylon membrane (Figure 5.1 A). 5mC was detected in all 4 time points, but remained constant over time with no increase or decrease in the methylation status of the T or UT parasites (Figure 5.1). This is similar to the co-inhibition study done on AdoMetDC/ODC (Van Brummelen, 2009).

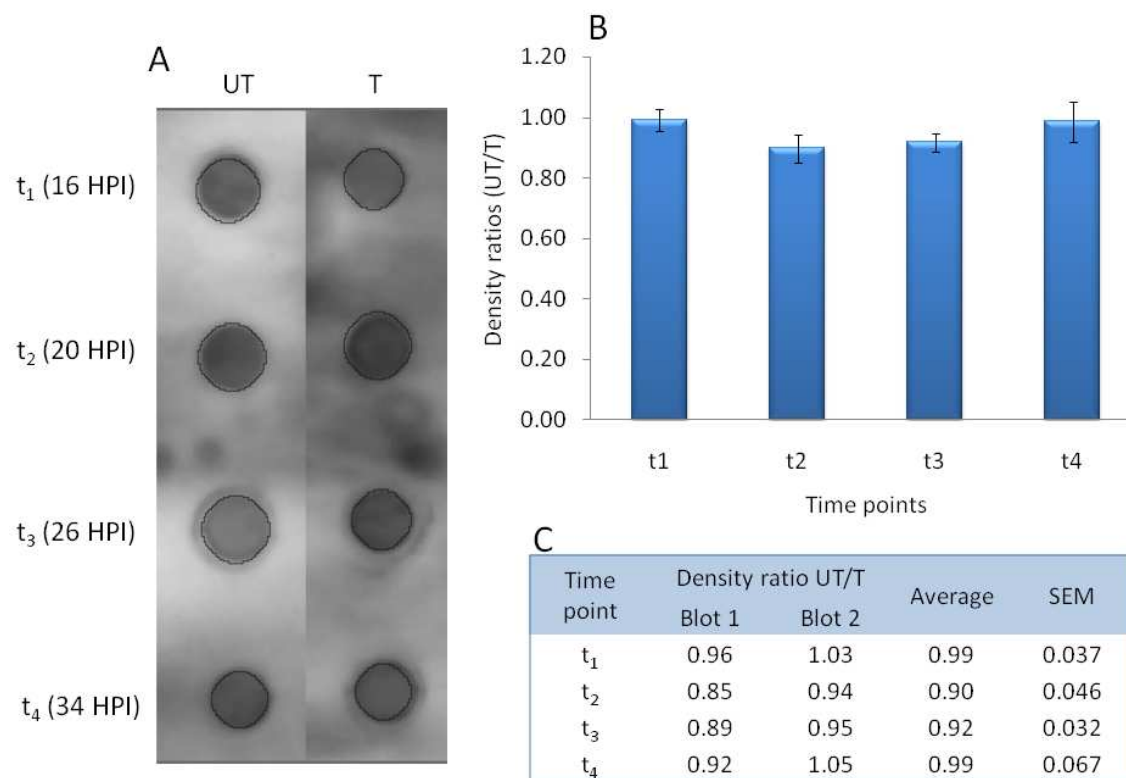


Figure 5.1: Determination of gDNA methylation (5mC) in AdoMetDC inhibited parasites.

A: Immunoblot of quantitatively loaded gDNA from treated and untreated parasites over time. B: Density ratios of the four time points investigated, error bars are representative of SEM for 2 experiments. C: Table containing the data from the immunoblots. Average ratios of 2 individual biological replicates and blots. SEM is representative of standard error of the mean. Data were calculated from the density determined by Quantity One.

5.3.2 Determination of AdoMet and AdoHcy metabolite levels upon inhibition of AdoMetDC

The methylation status of an organism is usually controlled by the AdoMet:AdoHcy ratios (Goldberg et al., 1999), which prompted the determination of the AdoMet and AdoHcy metabolite levels in AdoMetDC inhibited parasites. The metabolite levels of AdoMet and AdoHcy, which is crucial in polyamine metabolism and methionine recycling, were determined by HPLC for 2 time points (t_1 : 16 HPI and t_3 : 26 HPI; Figure 5.2). No significant differential regulation of either AdoMet or AdoHcy could be determined when UT_{t_1} was compared to T_{t_1} or UT_{t_3} compared to T_{t_3} ($p < 0.05$). This is similar to the co-inhibition of AdoMetDC/ODC, in which no significant differential regulation of either AdoMet or AdoHcy could be determined (Van Brummelen, 2009). This is also in support of the previous results that determined that no hypermethylation is present within the parasites (Section 5.3.1 and Van Brummelen 2009).

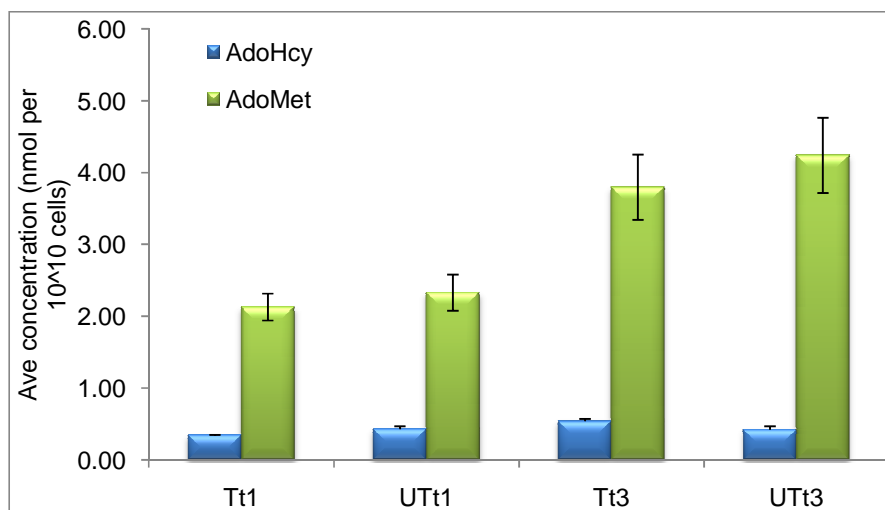


Figure 5.2: Metabolite levels of AdoMet and AdoHcy after AdoMetDC inhibition.

N=2 (biological replicates) and N=3 (technical replicates) for each time point. Error bars are representative of SEM, cells are normalised to the average cells per 10^{10} cells. t_1 is 16 HPI, t_3 is 26 HPI.

5.3.3 Polyamines and the folate pathway

It was determined in Chapter 4 that AdoMetDC inhibition resulted in decreased transcript abundance of various folate-related transcripts which therefore prompted further investigation. Folate depletion may result in an imbalance in AdoMet levels and ultimately an imbalance in polyamine biosynthesis (Bistulfi *et al.*, 2009). The effect of folate-free media and simultaneous inhibition of polyamines with MDL73811 were investigated using the MSF assay (Figure 5.3). The physiological concentration of folic acid in human erythrocytes is 23 nM (Nduati et al., 2008). In the presence of folate-free media the parasites had ~70% growth (therefore ~30% growth reduction) when compared to parasites in normal media (which is representative of 100% parasite growth)(Figure 5.3). The addition of 1 μ M MDL73811 (IC_{50}) to the folate-free media and normal

media was done to determine the effect of simultaneous folate depletion and AdoMetDC inhibition on the growth of the parasites. Treatment with 1 μM MDL73811 in folate containing media resulted in 50% parasite inhibition (Figure 5.3) with is similar to the IC_{50} of MDL73811 which has already been determined previously (Chapter 3). Similarly, when parasites were treated with 1 μM MDL73811 in the presence of 2.3 μM folates 50% parasite inhibition was determined. When folate depleted media were supplemented with 2.3 μM folates growth was restored to about 75%. Parasites exposed to folate-free media and 1 μM MDL73811 had a $\sim 75\%$ reduction in parasite growth (Figure 5.3). This is also a 25% reduction in parasite growth when compared to 1 μM MDL73811 (IC_{50}) in folate containing media. Therefore, the combination of folate depletion and AdoMetDC inhibition with MDL73811 resulted in a further 25% reduction in parasite growth when compared to MDL73811 alone and therefore prompted an investigation in to possible synergistic mechanisms between folate depletion and AdoMetDC inhibition.

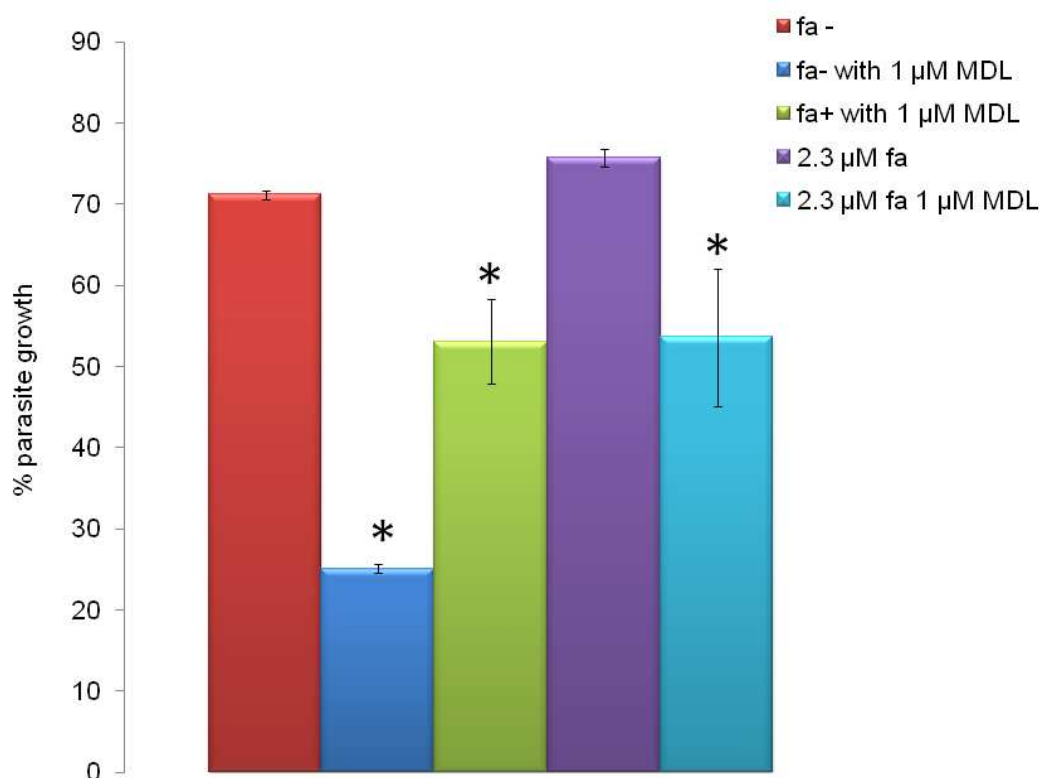


Figure 5.3: The combined influence of folate-free media and the irreversible AdoMetDC inhibitor MDL73811 on Plasmodial parasites.

MSF assay done in various concentrations of folic acid or folate free media but not pABA free media together with 1 μM MDL73811 at each concentration of folic acid. Data is representative of 2 biological replicates that were done in triplicate. Error bars are representative of SEM. Fa is folic acid. MDL is MDL73811. No fa is done in folate free, but not pABA free media without addition of folic acid to the media. A positive control is always included and is parasites in normal RPMI1640 media, and as a negative control, CQ is added to the parasites. * is indicative the treated sample compared to folate depleted samples with the student t-test $p < 0.05$.



The decreased parasite growth of the combination of AdoMetDC inhibition and folate depletion observed in Figure 5.3 prompted an investigation into possible synergistic interactions as a result of the combination of AdoMetDC inhibition and folate depletion. To further investigate this possibility, complete depletion of folates was desired for an effective experiment. Folate-free media still contained pABA that can be salvaged and utilised by *Pf*DHPS-HPPK for the production of folates. Therefore, the bifunctional enzyme DHFR-TS which is down-stream of DHPS-HPPK, and is responsible for folate production within the parasite was inhibited with PYR in an attempt to minimise pABA or folate salvage from the folate-depleted media. The IC_{50} of both PYR and MDL73811 in the presence and absence of folates were determined (Figure 5.4 A and B).

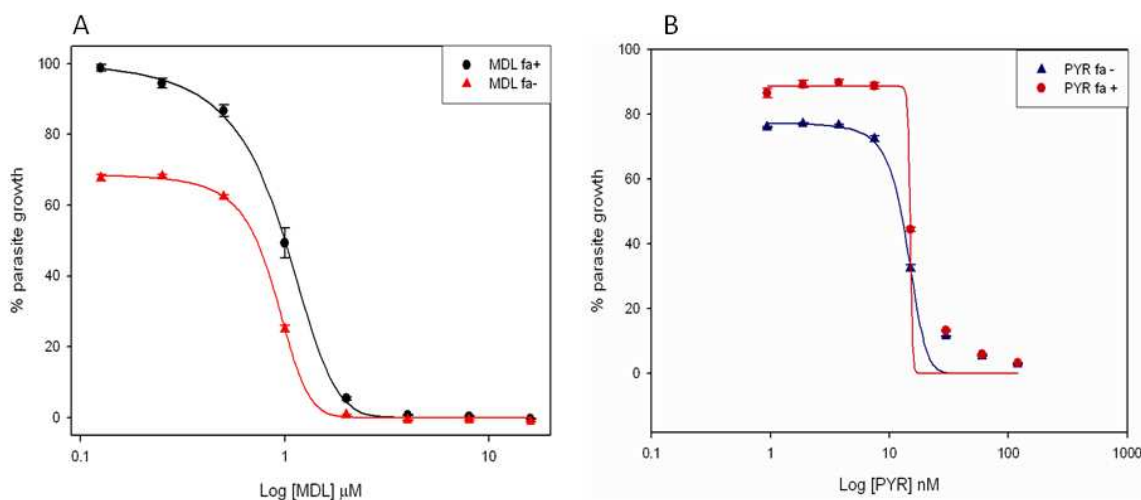


Figure 5.4: A dose response curve for the IC_{50} determination of MDL73811 and PYR in the presence and absence of folate free media.

(A) Error bars are representative of the SEM for 2 or 4 individual experiments done in triplicate. For folate free media (fa-) the $R^2=0.9990$ and IC_{50} is 0.8979μ M with SEM representative of 4 experiments. For folate containing media (fa+) $R^2=0.9908$ and the IC_{50} is 0.9600μ M. (B) Error bars are representative of the SEM for 2 individual experiments done in triplicate. For folate free media (Fa-) the $R^2=0.9926$ and IC_{50} is 14.1370 nM. For folate containing media (fa+) $R^2=0.9922$ and the IC_{50} is 15.0031 nM.

The IC_{50} of PYR remained unchanged in both the presence and absence of folates (Figure 5.4 B). In the presence of folate-containing media the IC_{50} of PYR in the *Pf*3D7 strain were determined to be 15 nM, while in the absence of folate the IC_{50} of PYR was determined as 14.1 nM. The IC_{50} of MDL73811 in normal folate-containing media was determined as 0.96μ M, while in the absence of folates within the media the IC_{50} of MDL73811 was determined as 0.89μ M (Figure 5.4 A).

In order to determine if complete inhibition of folates had a synergistic effect on AdoMetDC inhibition, parasites were inhibited with both PYR and MDL73811 at varying concentrations. The dose response curve for the co-inhibition of parasites with both PYR and MDL73811 shifted to the left indicating possible synergistic effects of the 2 drugs in combination (Figure 5.5). For

antagonism the combination curve would have shifted to the right of the individual curves, and for additivity the combination curve would have been in the middle of the 2 individual curves (Van Brummelen, 2009, Fivelman *et al.*, 2004). Indeed, the IC₅₀ of PYR changed from 14.1 nM to 7.3 nM in the presence of MDL73811, indicative of almost 50% reduction in IC₅₀-concentration needed for inhibition. This was not seen with MDL73811 for which the IC₅₀ remained almost unchanged in the presence and absence of PYR.

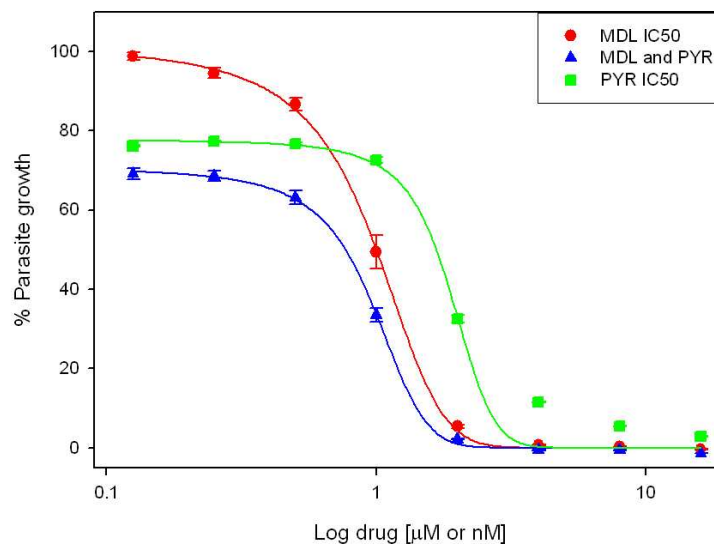


Figure 5.5: A dose response curve for the determination of possible interactions between MDL73811 and PYR in the absence of folates.

Error bars are representative of the SEM for 2 individual experiments done in triplicate. IC₅₀ of MDL73811 alone is 0.9600 µM. IC₅₀ of PYR alone is 14.1370 nM. In combination of both MDL73811 and PYR the IC₅₀ of MDL73811 is 0.9709 µM and the IC₅₀ of PYR is 7.2819 nM. The shift of the combination of drugs to the left is a possible indication of synergism/additive.

The determination of synergistic drug interactions depends on the methods chosen for investigation (Bonapace *et al.*, 2002). Time-kill analysis can be used to determine drug interaction in bacteria and is measured in time and log cfu/ml (Leonard *et al.*, 2008). However, the FIC measure is most commonly used (Equation 5.1) (Vivas *et al.*, 2007). Synergy between two drugs can be defined as $FIC \leq 0.5$, additivity/indifference is defined $FIC > 0.5$ to 4, and antagonism is defined as an $FIC < 4$ (Fivelman *et al.*, 2004, Hu *et al.*, 2002).

Calculation of the FIC of both PYR and MDL73811 resulted in a FIC value of 1.53 which is indicative of additivity (Fivelman *et al.*, 2004, Hu *et al.*, 2002). This is in contrast to the results obtained from the dose response curves that indicated possible synergism. This lack of possible synergism may be due to the lack of AdoMet:AdoHcy regulation as was determined in Section 5.3.2.

5.3.4 Methionine perturbation of parasites

Knowledge of stress responses can be useful in the elucidation of possible new drug targets, as these would be genes that should rather be avoided within this drug development process. Here, an attempt is made to induce stress responses upon the parasites in an effort to determine such stress genes particularly within polyamine metabolism. Transcripts that were specifically affected by AdoMetDC inhibition as was determined in Chapter 4 were selected to determine a polyamine specific or non-specific response. Primers were designed of transcripts affected to complement some of the already existing polyamine specific primers (Table 5.1 and Table 5.2).

Table 5.2: Additional primers designed for determination of polyamine specificity

PlasmoDB ID	Set	Primer sequence (5' - 3')	Product length	T _m (°C)
MAL13P1.214	PEMT f	ACA TTC CTG GAA AAT AAT CAA TAT AC	168	55.3
	PEMT r	TCC TAA ACC AGA TCC GAT ATC		
PF11_0061	Histone H4 f	GCA AGA AGA GGT GGT GTT AA	170	55.3
	Histone H4 r	CCT TGT CTT TTT AAG GAG TAT AC		
MAL13P1.56	M1-AP f	GGC AAA ATA TGA CGT TAC AGT AAC	162	57.6
	M1-AP r	CCA GCT ACA ACA GCA AAT AAA TAA		
PFE1050w	AHC f	AGA GCT ACC GAT TTT TTA ATA TC	155	53.5
	AHC r	CCT TCC ATT ACA GCT TGT ATA G		
PFF1300w	Pyruvate kinase f	TTG GCA CAA AAA TTG ATG ATA TC	166	53.5
	Pyruvate kinase r	CTG AAA GCA TAA CAC AAT CAG TAC		

Morphological evaluation of the addition of the 4 different Met concentrations to the *Pf3D7* parasites revealed that in the presence of 0.1 mM, 1mM and 10 mM Met there is no visible morphological difference between the T_{met} and UT_{met} parasites. It does seem morphologically that the parasites treated with 100 mM Met are morphologically smaller than the other parasites at the trophozoite stage (Figure 5.6).

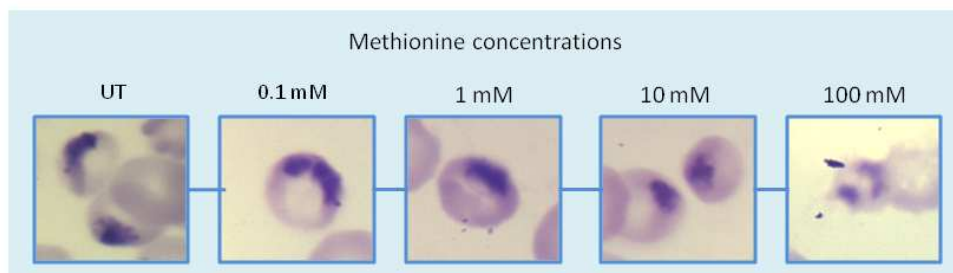


Figure 5.6: Morphological illustration of the various methionine concentrations on the parasites. Methionine was added in the early ring stage and the parasites were harvested 24 h later in the trophozoite stage.

The addition of Met had an influence on transcripts involved in polyamine metabolism similar to the inhibition of AdoMetDC with MDL73811 (Chapter 4). High concentrations of Met (100 mM) induced decreased transcript abundance of AdoMet synthase, AHC, HH4 and PEMT which was similarly determined with AdoMetDC inhibition with MDL73811 (Chapter 4). Transcripts with increased transcript abundance were LDC and arginase (Figure 5.7). In contrast to the high Met concentration that induced possible polyamine specific transcripts, the lower concentrations of methionine resulted in unchanged transcripts for all of the transcripts that were investigated. This may support the notion that AdoMet synthesis within the parasite may be homeostatically controlled and is under tight regulation possibly independent of polyamine metabolism.

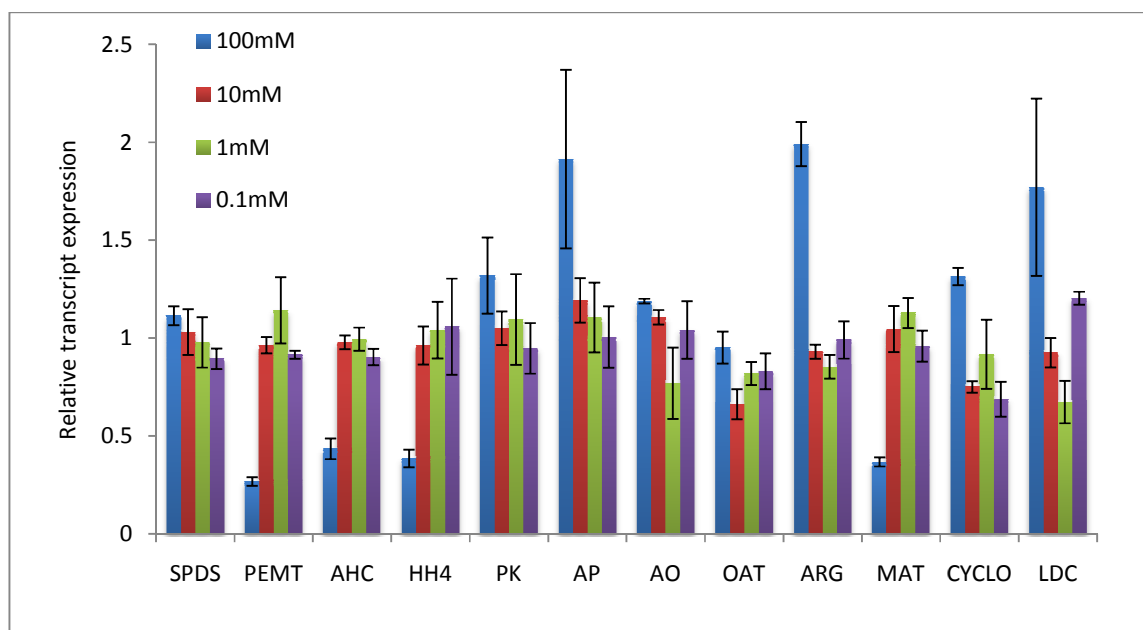


Figure 5.7: qRT-PCR of methionine treated parasites.

N=2 error bars representative of the SEM. All transcripts normalised to LDH. SPDS: spermidine synthase, PEMT: phosphoethanolamine N-methyltransferase, AHC: adenosylhomocysteinase, HH4: histone H4, PK: pyruvate kinase, AP: M1-family aminopeptidase, AO: AdoMetDC/ODC, OAT: ornithine aminotransferase, ARG: arginase, MAT: AdoMet synthase, CYCLO: cyclophilin, LDC: lysine decarboxylase.

5.3.5 Comparison of transcriptomic and proteomic data

Comparison of the transcriptomic and proteomic data revealed that 16 transcripts were similarly detected as proteins in the proteomic investigation (Table 5.3 and Figure 5.8). Therefore, 3% (16/549) of the transcripts that were identified as differentially regulated and 26% (16/61) of the differentially affected identified proteins were shared between the 2 technologies employed.

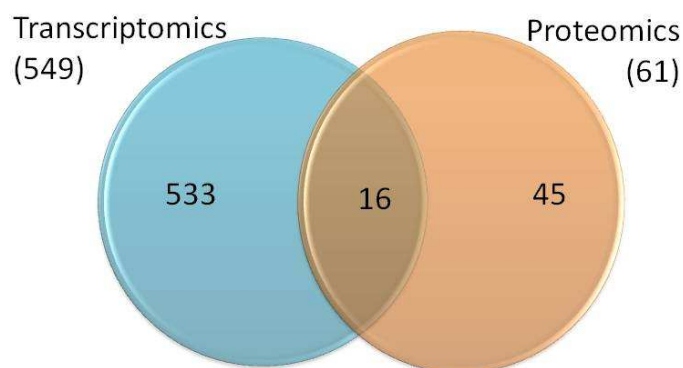


Figure 5.8: Venn diagram of similarities between the transcriptomic and proteomic data sets for the AdoMetDC perturbation.

In total 549 transcripts were determined to be differentially affected by AdoMetDC inhibition. In total, 61 unique protein groups were identified to be differentially regulated, when the 1-DE and 2-DE results were combined as a total proteomic study.

Of the 16 shared transcripts and proteins that were identified, 8 had a similar decreased abundance in both the transcript and protein (Table 5.3). Three proteins had multiple isoforms that were both increased and decreased in abundance and therefore not always similar to the transcript data and include MAL13P1.214, PF10_0155 and PFF1300w. Five proteins had increased protein abundance but had decreased transcript abundance (Table 5.3). These results are indicative of transcriptional and translational regulatory mechanisms within the parasite.

Table 5.3: Similar transcripts obtained for both the transcriptomic and proteomic data.

PlasmoDB ID	Name	Proteomics		Transcriptomics
		FC Tt ₁	FC Tt ₂	FC Tt ₃
Decreased abundance				
PF14_0138	hypothetical protein		-3.3	-1.8
PF14_0187	glutathione S-transferase	-1.6		-1.8
PFI1090w	s-adenosylmethionine synthetase, putative	-1.3		-2.3
PFI1270w	PFI1270w	-3.3		-2.9
PFL2215w	Actin		-1.4/-2.0	-2.5
PF11_0061	Histone H4, putative*	-5.0/-3.4		-3.4
PF11_0062	Histone H2B*	-5.0/-3.4		-2.9
PFE0165w	Actin depolymerising factor, putative*	-4.4		-2.2
Increased abundance				
MAL13P1.283	TCP-1/cpn60 chaperonin family, putative	1.3		-1.7
PF08_0054	heat shock 70 kDa protein	2.7	2.7	-1.9
PF13_0141	L-lactate dehydrogenase	1.5	3.1	-1.9
PFE0660c	purine nucleotide phosphorylase, putative	1.6		-3.0
PFL1420w	Macrophage migration inhibitory factor homolog, putative*	0.9		-2.1
Multiple isoforms				
MAL13P1.214	phosphoethanolamine N-methyltransferase, putative	-1.5	1.7/-3.8/ -1.8	-5.0
PF10_0155	Enolase	2.0/-4.1	1.4	-2.7
PFF1300w	pyruvate kinase, putative	1.3/-1.3	2.3	-1.7

Multiple entries for the proteomics data is separated by a dash, which is representative of various isoforms *Proteins identified for SDS-PAGE only.

Some of the polyamine specific proteins that were identified by MS/MS in Chapter 3 were compared to their transcript profiles that were obtained in Chapter 4. The fold change of the MDL73811-treated *Pf3D7* parasites were plotted for both the transcripts (t_1 to t_3) as well as the proteins (t_1 to t_2) to determine possible regulatory mechanisms (Figure 5.9).

Adenosine deaminase (PF10_0289), AdoMet synthase (PFI1090w) and PNP (PFE0660c) all had transcript and protein abundance that decreased similarly over time, although it did seem that the protein abundance of adenosine deaminase (PF10_0289) does lag behind the transcript abundance in Tt_2 (Figure 5.9). This lag was also determined for Hsp70 (PF08_0054) which revealed a high protein abundance when compared to the transcript abundance although the protein abundance was slowly decreasing and therefore, also had a delay between transcript and protein abundance. Finally, it was determined that eIF5A (PFL0210c) had decreased transcript and protein abundance although the protein abundance was decreased dramatically from that of the transcript abundance (Figure 5.9). PEMT (MAL13P1.214) and enolase (PF10_0155) both had decreased transcript levels, but had various protein isoforms that were identified. Three protein isoforms were detected for PEMT (MAL13P1.214) of which 2 of these protein isoforms had decreased protein abundance similar to the transcript levels, with the other protein isoforms having increased protein abundance levels. Similarly for enolase (PF10_0155) 1 protein isoform had decreased protein levels but was lagging behind the transcript while the other protein isoform had increased protein abundance. Pyrroline-5-carboxylate reductase (MAL13P1.284) had unchanged transcript levels (+1-fold), but the protein abundance increased from Tt_1 to Tt_2 . Similarly, 2-cys peroxiredoxin (PF14_0368) and Hsp60 (PF10_0153) also had unchanged transcript levels (-1-fold) that remained constant over the 3 time points with the protein abundance that also increased from Tt_1 to Tt_2 . A decrease in transcript abundance with an increase in protein abundance was determined for GST (PF14_0187) and pyruvate kinase (PFI1300w).

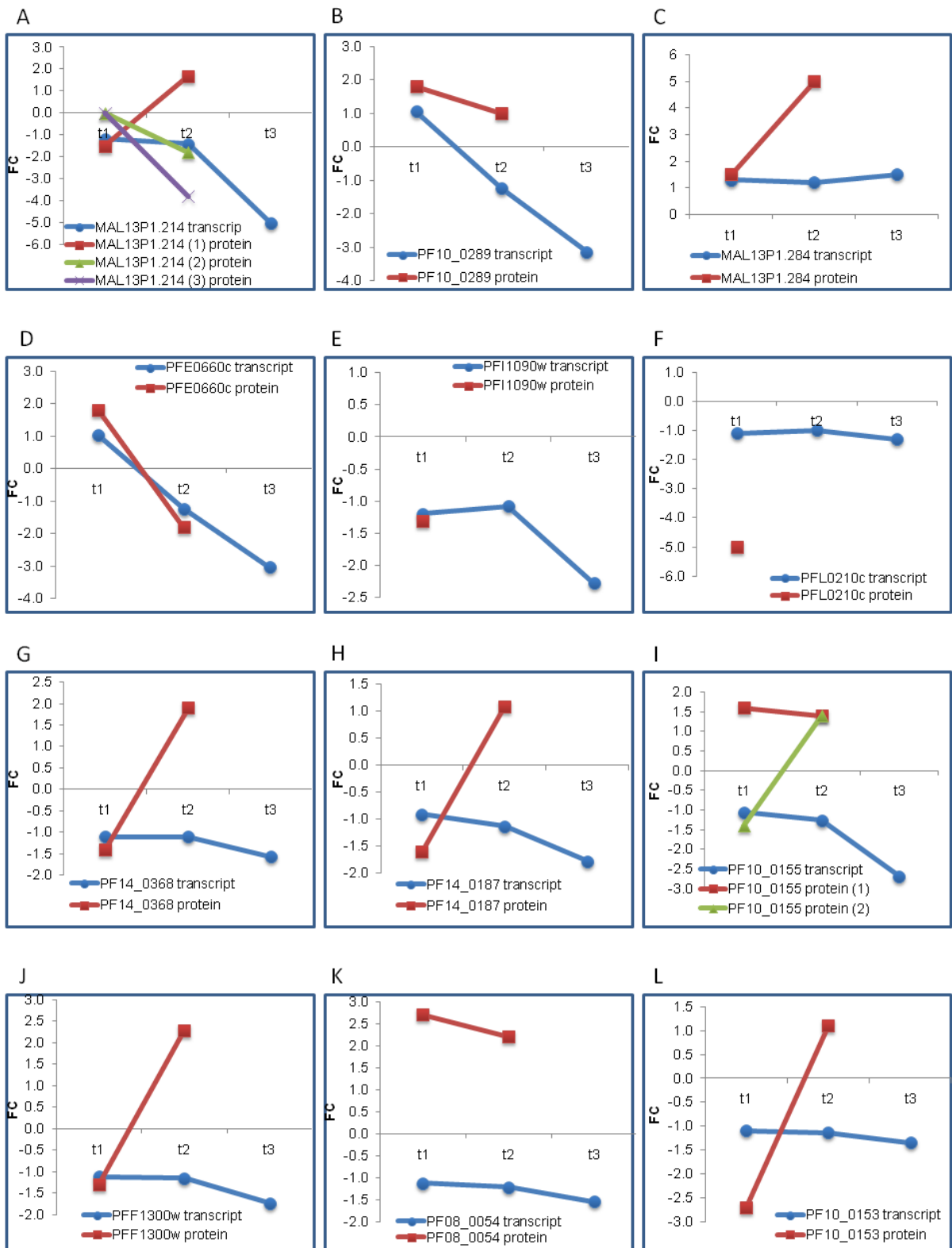


Figure 5.9: Correlation between transcript and protein abundance

A: phosphoethanolamine N-methyltransferase, B: adenosine deaminase, C: Pyrroline-5-carboxylate reductase, D: purine nucleotide phosphorylase, E: S-adenosylmethionine synthetase, F: Eukaryotic initiation factor 5a, putative, G: 2-Cys peroxiredoxin, H: Glutathione s-transferase, I: enolase, J: pyruvate kinase, K: heat shock protein 70 kDa, L: heat shock protein 60 kDa.

5.4 Discussion

Inhibition of AdoMetDC with MDL73811 resulted in the identification of gDNA methylation but no hypermethylation could be identified. MDL73811 inhibition of Trypanosome AdoMetDC revealed hypermethylation of nucleic acids and proteins, and concurrent parasite death due to the accumulation of AdoMet and subsequent interference with translational processes (Bacchi *et al.*, 1992a, Goldberg *et al.*, 1997a). Similar results of hypermethylation was obtained in the liver of rats fed with excess methionine (Bacchi *et al.*, 1995). Hypermethylation of promoter genes and an increase in the mRNA expression of DNA methyltransferases is commonly associated with cancerous cells, although the correlation between DNA methylation and the mRNA expression of DNA methyltransferases are not always clear (Oh *et al.*, 2007, Park *et al.*, 2006). Hypermethylation is associated with various malignancies (Oh *et al.*, 2007) and usually occurs in cancerous cells in which epigenetic control is the result of hypermethylation of the tumour suppressor genes (Chan *et al.*, 2008). Gene silencing is commonly associated with the occurrence of hypermethylation of genes (Chan *et al.*, 2008), although epigenetic control through 5mC methylation in Plasmodial parasites are contradictory (Choi *et al.*, 2006). Previously, it was determined that 5mC does not occur in Plasmodial parasites (Choi *et al.*, 2006). In contrast to these results, it was determined within this study that 5mC does exist within the Plasmodial parasites and that this 5mC does increase over time as the parasite progress through its life stages. In contrast to MDL73811 inhibition of AdoMetDC in Trypanosomes, hypermethylation was not detected with the inhibition of *PfAdoMetDC* with MDL73811. This also corroborate with the lack of hypermethylation as determined in the co-inhibition of *PfAdoMetDC/ODC* with MDL73811 and DFMO (Van Brummelen, 2009).

The AdoMet and AdoHcy metabolite levels were determined using HPLC in two different time points. It was observed that the AdoMet level does increase over time from 16 HPI to 26 HPI, but that this increase in AdoMet levels is similar in both the treated and untreated parasites. No significant changes could be detected in the AdoHcy metabolite levels. AdoMet plays an integral role in the production of polyamines and acts as a methyl donor for nearly all methylation reactions that include DNA and protein methylation. AdoHcy is the product formed after the methylation reaction and is rapidly degraded by AHC since high concentrations of AdoHcy is toxic to the parasite and will also result in down-regulation of the methyltransferases (Nakanishi *et al.*, 2001). Therefore, the AdoMet:AdoHcy ratio is of importance within the parasites as this may result in hyper- or hypomethylation of DNA within the parasite. The transcript abundances of both AdoMet synthase and AHC were decreased as well as the protein abundance of AdoMet synthase. The unchanged metabolite levels of both AdoMet and AdoHcy together with decreased transcript and



protein abundances of AdoMet synthase and AHC may be a reason for the lack of hypermethylation with AdoMetDC inhibition. This was similarly determined with the co-inhibition of AdoMetDC/ODC (van Brummelen *et al.*, 2009). It therefore seems that in Plasmodial parasites the methionine cycle is in homeostasis and maintains AdoMet levels at a constant level, due to the decreased transcript and protein abundances of AdoMet synthase and AHC. This once again brings into question the regulatory role of AdoMet synthase as possible regulator of the entire AdoMet cycle as well as transcriptional regulatory mechanisms of AdoMet synthase.

In Chapter 4 a possible link between polyamine biosynthesis and the folate pathway was established with the decreased transcript abundance of various folate-related genes (DHFR-TS, DHFS-FPGS, serine hydroxymethyl transferase, NDPK) as a result of AdoMetDC inhibition. These transcriptomic results together with a recent finding that further iterated that polyamine biosynthesis does impact on folate metabolism in prostate cells and that folate depletion will result in imbalanced AdoMet levels (Bistulfi *et al.*, 2009) prompted further investigation. The addition of MDL73811 in the absence of folates resulted in decreased parasite growth when compared to MDL73811 inhibition in media that does contain folates. To further establish a possible link between polyamines and folates the IC_{50} 's of both PYR and MDL73811 was determined in the presence and absence of folates. The IC_{50} of PYR remained unchanged regardless of the media used, but unlike PYR, the IC_{50} of MDL73811 was slightly reduced in the absence of folates. This prompted the determination of possible synergy determination between polyamine and folate depletion especially since a synergistic killing effect was established in human ovarian cancer cell lines depleted of both folate and polyamines (Marverti *et al.*, 2010). Although the combination of folate depletion and polyamine depletion resulted in reduced IC_{50} 's of both PYR and MDL73811, it was established that PYR and MDL73811 does not seem to act synergistically but rather have an additive effect, although further investigation is needed to confirm this. The lack of synergy between polyamine and folate depleted parasites may be due to the tight regulation of AdoMet levels that remained unchanged within MDL73811-treated parasites. Folate depletion of human cells impacts on the AdoMet pool and may result in epigenetic damage (Pogribny *et al.*, 1995). N-5-methyl THF is essential in the recycling of homocysteine back into methionine and THF. Low folate as a result of decreased folate-related transcripts with the inhibition of AdoMetDC may therefore prevent the recycling of homocysteine into methionine and ultimately AdoMet (Pogribny *et al.*, 1995, Sohn *et al.*, 2003).

Met is important in protein synthesis and the production of AdoMet (Reguera *et al.*, 2007). The addition of Met had an influence on transcripts involved in polyamine metabolism similar to

MDL73811. Both MDL73811 and Met resulted in a decrease of transcript levels for PEMT, AHC and histone H4. Met is essential for protein synthesis but also as substrate for the production of AdoMet which is crucial for polyamine biosynthesis and transmethylation reactions (Goldberg *et al.*, 2000, Bacchi *et al.*, 1995). Met is present in low levels and supplementation with Met may be optimal for parasite growth (Liu *et al.*, 2006). Met is needed for the initiation of protein synthesis, polyamine synthesis, and is the precursor for AdoMet via AdoMet synthase within polyamine metabolism. Notably, it was determined that with the addition of high Met concentrations, the transcript level of AdoMet synthase was decreased similar to inhibition of AdoMetDC with MDL73811. This indicates that AdoMet synthase may become saturated with Met, and in response induce transcriptional repression of the enzyme. This was not seen at lower Met concentrations. Excess levels of methionine can suppress the methylation cycle by causing a reduction in the AdoMet:AdoHcy ratio, that inhibits transmethylation reactions (Dunlevy *et al.*, 2006). This may be a reason for the lack of hypermethylation with inhibition of AdoMetDC in Plasmodial parasites. Therefore, the similarities observed for the addition of high Met concentrations and the inhibition of AdoMetDC with MDL73811 could indicate that AdoMet synthase is transcriptionally regulated by Met, similar to the regulation of Plasmodial phosphoethanolamine N-methyltransferase by choline (Witola & Ben Mamoun, 2007).

Comparison of the transcriptomic and the proteomic studies revealed that only 16 proteins were identified with both technologies. This low number is probably due to the large amount of transcripts that can be identified with the use of microarrays compared to 2-DE in which far less proteins could be identified. Comparison of the transcript and protein abundances for the shared proteins revealed some interesting observations. *T. cruzi* metabolism is mainly controlled by post-transcriptional and post-translational control (Clayton, 2002, Carrillo *et al.*, 2007, Kahana, 2007), while previously it was reported that *P. falciparum* is mainly controlled by post-transcriptional regulation and that there is generally good correlation between mRNA and protein levels (Le Roch *et al.*, 2004). This was not always the case with the inhibition of AdoMetDC, which did reveal correlation between transcript and protein abundances of some of the proteins but it seemed that the majority did not correlate well. This corroborate with the notion that mRNA abundance is not always proportional to protein expression due to post-transcriptional modifications, RNA splicing, post-translational modifications, protein degradation, protein turnover as well as differences between transcription and translation (Hegde *et al.*, 2003, Griffin *et al.*, 2002, Gygi *et al.*, 1999).

Various studies have been employed to determine the correlation between mRNA and protein abundance in which most found a lack of correlation between mRNA and protein abundance



(Anderson & Seilhamer, 1997, Gygi et al., 1999, Chen et al., 2002). In a study on *S. cerevisiae* the correlation of 678 loci were determined and also demonstrated poor correlation between mRNA and protein expression ratios (Washburn *et al.*, 2003). The majority of deviation was from the protein abundance that was altered but had unchanged mRNA. Interestingly, methionine metabolism had an almost perfect correlation between mRNA and proteins expression (Washburn *et al.*, 2003).

The regulation of mRNA half life is an important determination of gene expression levels and is essential for regulation of post-transcriptional control. The average mRNA decay half-life in *P. falciparum* increases with the progress of the parasite through its life cycle (Shock *et al.*, 2007). The average mRNA half-life of ring stage parasites is 9.5 min, which progressively increases to 20.5 min in trophozoites and 65.4 min in late schizonts. The cascade of gene expression seen in *P. falciparum* is unlike any other organism, and may provide clues that post-translational regulation may be a key in gene regulation although little is known on the regulation of this cascade or how it is maintained (Shock et al., 2007). mRNA abundance is the result of the rate at which mRNA is produced minus the rate at which it is decayed, with mRNA decay a extremely well regulated process rather than the degradation of all transcripts (Wang *et al.*, 2002). mRNA decay may also be related to protein function and the energy requirements of the growing parasites (Wang *et al.*, 2002, Garcia-Martinez *et al.*, 2004).

The inhibition of AdoMetDC with MDL73811 resulted in the identification of a few major groups regarding the correlation between transcript and protein abundance levels. The first group revealed that a change in the transcript levels was similarly seen in the protein levels and may therefore correlate to possible transcriptional mechanisms (Chen *et al.*, 2002). Basically, most of the transcripts displayed a decrease in transcript abundance which was similarly determined with a decrease in protein abundance although the decrease in protein abundance was sometimes associated with a delay. Proteins in this group included adenosine deaminase, AdoMet synthase, PNP, Hsp70, and eIF5A. The similarity of the transcript and protein abundance of *PfeIF5A* differ from that of eIF5A in lung adenocarcinomas in which mRNA and protein abundance did not correlate due to higher protein expression indicative of a post-transcriptional or post-translational regulation mechanism (Chen *et al.*, 2003). It may therefore be that *PfeIF5A* may be under transcriptional regulation or that it has other isoforms which has not yet been identified on the 2-DE gel and may therefore result in a change in protein abundance. The delay of the protein abundance that is observed in some of these proteins may be due to a delay in protein turnover, or slow degradation of the protein (Foth *et al.*, 2008). Post-transcriptional regulation may be a major mechanism of gene expression in *P. falciparum* since it is carried out by chromatin remodelling in

the various life stages (Ponts *et al.*, 2010). The ring stage plays an essential role in the regulation of gene expression since stress in the ring stage can initiate gametocytogenesis (Ponts *et al.*, 2010). Transcriptional regulation may also be mediated by co-regulation of genes through copy number variant regions that may play a role in gene regulation to genes that are distant from them (Mackinnon *et al.*, 2009). Overall, the process of transcription in *P. falciparum* is highly coordinated and co-regulation of transcription of adaptive genes may play a role in the ability of the parasite to adapt to environmental stresses (Mackinnon *et al.*, 2009).

Another group that was identified were proteins that revealed a decrease in transcript abundance but had an increase in protein abundance and included pyruvate kinase, MAL13P1.283, and GST. This may be due to some mechanism of translational repression, or protein turnover, or it may be that these proteins have various PTM's that have not yet been identified on the 2-DE gel and that these protein isoforms may resemble the transcript abundance (Foth *et al.*, 2008). It may also be due to a process of post-transcriptional gene silencing which seems to play a role in gene expression through translational repression (Hall *et al.*, 2005). Translational repression and mRNA turnover plays an important role in stage specific gene expression of the malaria parasite and therefore also has a key role in parasite development (Mair *et al.*, 2006).

2-Cys peroxiredoxin, pyrroline 5-carboxylate reductase, Hsp60 and 40S ribosomal protein all formed part of a group that revealed no change in transcript levels but an increase in protein abundance which is probably due to post-transcriptional regulation (Hegde *et al.*, 2003). Another possibility may be due to slow degradation or that the proteins may be resistant to degradation, or perhaps the protein lag behind the transcript and the decrease in protein abundance will be seen later (Foth *et al.*, 2008). This may also be similar to *PfDHFR-TS* which is translationally regulated as it is able to bind to its own mRNA, therefore initiating the inhibition of its own translation (Zhang & Rathod, 2002). In the presence of an inhibitor, *PfDHFR-TS* has no change in transcript level but has an increase in protein expression therefore releasing the translational restraints upon the protein (Nirmalan *et al.*, 2004b). It may therefore be concluded that upon inhibition of AdoMetDC and subsequent polyamine depletion 2-cys peroxiredoxin, pyrroline 5-carboxylate, hsp60 and 40S ribosomal protein may all be translationally regulated.

PEMT and enolase both had decreased transcript levels but had multiple protein isoforms. Some of the protein isoforms resembled the transcript abundance while other protein isoforms increased in protein abundance. This reveals some mechanisms of PTM's where different protein isoforms may have different functions (Foth *et al.*, 2008, Pal-Bhowmick *et al.*, 2007). Phosphoethanolamine N-



methyltransferase is expressed throughout the life cycle of *P. falciparum* (Pessi *et al.*, 2004). It is a monomeric enzyme with a single catalytic domain of which the activity is inhibited by its own product phosphocholine (Pessi *et al.*, 2004). PEMT is regulated by metabolite-mediated transcriptional regulation and subsequently degraded by proteasomal regulation (Witola & Ben Mamoun, 2007), although the various post-translational modifications on the protein isoforms cannot be excluded and are often associated with differences that arise between the protein and mRNA abundance due to separate regulation of the multiple isoforms (Chen *et al.*, 2002).

Overall, it seems that upon polyamine depletion due to the inhibition of AdoMetDC in Plasmodial parasites the majority of regulatory mechanisms are controlled by post-transcriptional regulatory mechanisms. Post-translational modifications were also abundant in the proteome (Chapter 2 and 3) and may therefore also play a role in the regulation of protein isoforms. It can also be concluded that various post-transcriptional regulatory mechanisms exist and that combinations of these regulatory motifs regulate gene expression similar to previous reports (van Noort & Huynen, 2006).